

All reagents and organic dyes, unless otherwise noted, were obtained from the Energy Chemical and used without further purification. The solvents (ethanol, *o*-dichlorobenzene, 1,4-dioxane, mesitylene and *n*-butanol) for COF synthesis condition optimization were purchased from Energy Chemical. Deionized water was used for the preparation of 6 M acetic acid. Solvents for removal of guests from the pores of COF were obtained from Sinopharm Chemical Reagent Beijing Co., Ltd.

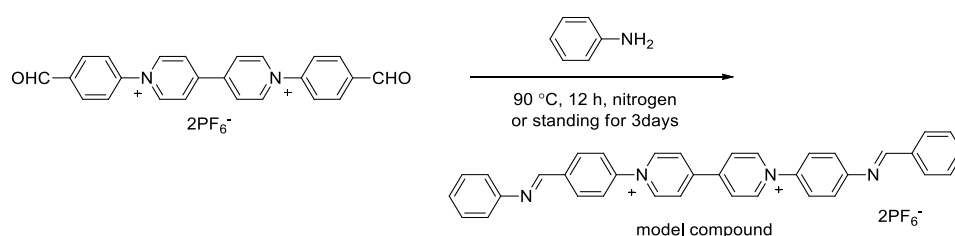
Methods: Powder X-ray diffraction measurements were carried out on a Bruker D4 ENDEAVOR X-Ray diffractometer (Bruker, Germany) at 40 kV and 40 mA with Cu K α radiation ($\lambda = 1.5406 \text{ \AA}$). Solid-phase synchrotron X-ray-scattering experiments were performed on the BL16B beamline of Shanghai Synchrotron Radiation Facility, using a fixed wavelength of 0.124 nm, a sample-to-detector distance of 1.84 m and an exposure time of 200 s. The 2D scattering pattern was collected on a charge-coupled device camera, and the curve intensities versus q were obtained by integrating the data from the pattern. Small-angle X-ray scattering experiments were conducted both on the NanoStar U SAXS System (Bruker, German) using Cu K α radiation (40 kV, 35 mA) and exposure time of 2 minutes, and on the SAXSess mc2 system (Anton Paar, Austria) with Ni filtered Cu K α radiation source. The power of X-ray source was operated at 50 mA and 40 kV. The d-spacing values were calculated by the formula $d = 2\pi/q$. Scanning electron micrographs of the samples were obtained on a Nova nano SEM 450 Field Emission Scanning Electron Microscope at 3.00 kV with the material adhered to the SEM sample holder directly or on a Phenom China Scanning Electron Microscope at 15.00 kV after the material that adhered to the sample holder was been gilded to 10^{-1} - 10^{-2} vacuum degree. Transmission electron micrographs were recorded on a JEM 2011 FETEM microscope at 200 kV aligned for low dose ($10 \text{ e } \text{\AA}^{-2} \text{ s}^{-1}$) diffractive imaging. TGA experiments were performed on a Model TGA/SDTA 851 instrument. Samples were placed in alumina pans and heated at a rate of 5 °C per minute from 100 to 900 °C under a nitrogen atmosphere. Fourier transform infrared spectroscopy was carried out with an Avatar-360 FT-IR spectrometer (Nicolet, USA). The samples for IR spectra were prepared as KBr pellets. Solid-state NMR spectra were recorded at ambient pressure on a Bruker 400WB AVANCE III spectrometer using a standard Bruker magic angle-spinning (MAS) probe with 4 nm zirconia rotors. UV-Vis spectra were performed on a Perkin-Elmer 750s instrument from 200-800 nm at the scan rate of 3 nm/ internal. Gas adsorptions of N $_2$ at -196 °C and CO $_2$ at 0 °C were measured on a Micromeritics Model ASAP 2020 gas adsorption analyzer. About 40 mg of activated sample was degassed at 180 °C for 10 h by using the “outgas” function of the surface area analyzer. Helium gas was used to estimate the dead volume. The saturation pressure (P_0) was measured throughout the N $_2$ analyses via a dedicated saturation pressure transducer, which helped to monitor the vapor pressure for each data point. For CO $_2$ isotherm measurements, activated sample was transferred into a pre-weighed glass sample tube. The tube was then sealed and quickly transferred to a system providing 10^{-4} torr dynamic vacuum. The sample was kept under this vacuum at 180 °C for 10 h and then used for CO $_2$ adsorption measurements.

Adsorption experiments. In a typical experiment, activated PC-COF was added to a solution of MO, AR-27, AG-25, DFBM, or IC of fixed concentration in water. The amount of PC-COF was calculated by assuming no defects. The UV-vis spectra of the solutions were recorded after shaking for different time

and standing for 15 minutes at room temperature. The absorption of the dye was then recorded and used to calculate the amount of dye that was absorbed by **PC-COF**.

Desorption experiments. In a typical experiment, MO-adsorbed **PC-COF** (5 mg) containing 8.9×10^{-6} mole of MO was immersed into a solution of ethanol (85 mL) and acetic acid (15 mL). The UV-vis spectra of the solution were recorded at 60 °C after shaking for different time and then standing for 15 minutes. The absorption of the acidized MO was recorded and used to calculate the amount of the acidized MO that was released from the MO@**PC-COF** sample.

TAPB and **BFBP**²⁺•2PF₆⁻ was synthesized according to the reported procedure.^{1,2} **BFBP**²⁺•2Cl⁻ was obtained from **BFBP**²⁺•2PF₆⁻ by ion-exchange with tetrabutylammonium chloride in acetonitrile. The precipitation was filtrated and washed with acetonitrile, and dried in vacuo to give **BFBP**²⁺•2Cl⁻ as a pale grey solid. **FBP**²⁺•2PF₆⁻ and **BFBP**²⁺•2Cl⁻ gave rise to the identical ¹H and ¹³C NMR in DMSO-d₆.



Synthesis of model compound 1,1'-bis(4-((E)-(phenylimino)methyl)phenyl)-[4,4'-bipyridine]-1,1'-diium: The model compound was synthesized by the reaction of **BFBP**²⁺•2PF₆⁻ (98 mg, 0.15 mmol) and aniline (28 mg, 0.30 mmol) in 10 mL acetonitrile under nitrogen at 90 °C for 12 hours or standing in atmosphere at r.t. for 3 days. Under the standing condition, the grey precipitate was collected and filtration was dried under vacuum to get the yellow powder. ¹H NMR (400MHz, DMSO-d₆): 9.77 (s, 4 H), 9.12 (s, 4 H), 8.87 (s, 2 H), 8.34 (s, 4 H), 8.15 (s, 4 H), 7.51-7.47 (t, 4 H), 7.39-7.37 (d, 4 H), 7.33 (s, 2H) ppm. ¹³C NMR (400 MHz, DMSO-d₆): 159.5, 151.2, 149.6, 146.34, 144.2, 139.1, 130.5, 129.8, 127.3, 127.1, 126.0, 121.7 ppm. HRMS (ESI): Calcd for C₃₆H₂₈N₄: 516.2314 [M-2Cl]²⁺. Found 516.2282.

Synthesis of PC-COF. 1,3,5-Tris(4-aminophenyl)benzene (**TAPB**) (42 mg, 0.12 mmol) and 1,1-bis(4-formylphenyl)-4,4'-bipyridinium dichloride (**BFBP**²⁺•2Cl⁻) (79 mg, 0.18 mmol) were weighed into a schlenk tube. To the mixture were added 3.6 mL o-dichlorobenzene and 0.4 mL ethanol as solvent combination and 0.8 mL aqueous acetic acid (6 M) as catalyst at the ratio 9:1:2. The schlenk tube was then flash frozen at 77 K (liquid N₂ bath) and degassed by three freeze-pump-thaw cycles. The tube was sealed off with a little N₂ in and then heated at 120 °C for 7 days. The powders formed were filtered out, and washed with ethanol and acetone, and then dried under vacuum at 120 °C for 12 hours to give **PC-COF** as a pale brown powder (0.10 g, 83% based on TAPB).

Synthesis of PC-COF-2. TAPB (14 mg, 0.04 mmol) and **BFBP**²⁺•2Cl⁻ (39 mg, 0.06 mmol) were weighed into a schlenk tube. To the mixture was added 1.5 ml o-dichlorobenzene and 0.5 ml ethanol as solvent combination and 0.35 ml 6 mol/L aqueous acetic acid as catalyst at the ratio 15:5:3.5. Then the schlenk tube was then flash frozen at 77 K (liquid N₂ bath) and degassed by three freeze-pump-thaw cycles. The

tube was sealed off with a little N₂ in and then heated at 120 °C for 7 days. After the reaction the COF powders are filtered out, washed with dichloromethane and acetone and then dried under vacuum at 120 °C for 12 hours to give **PC-COF-2** as a pale grey powder (40 mg, 73% based on **TAPB**).

Adsorption of dyes by PC-COF-2. Activated **PC-COF-2** (1.2 mg) were added to a solution of MO, IC, or AG-25 in 10 ml water to prepare solutions of required concentrations. The molar quantity of the anionic units of dyes was equal to that of the cationic unit of **PC-COF-2** (1.2 mg) with the assumption that the **PC-COF-2** was of non-defects. The UV-vis spectra of the solution were recorded after different shaking time at room temperature and at least 10-minute standing time. The decreased absorption of dyes was then used to calculate the amount of dyes that was absorbed by the **PC-COF-2** sample.

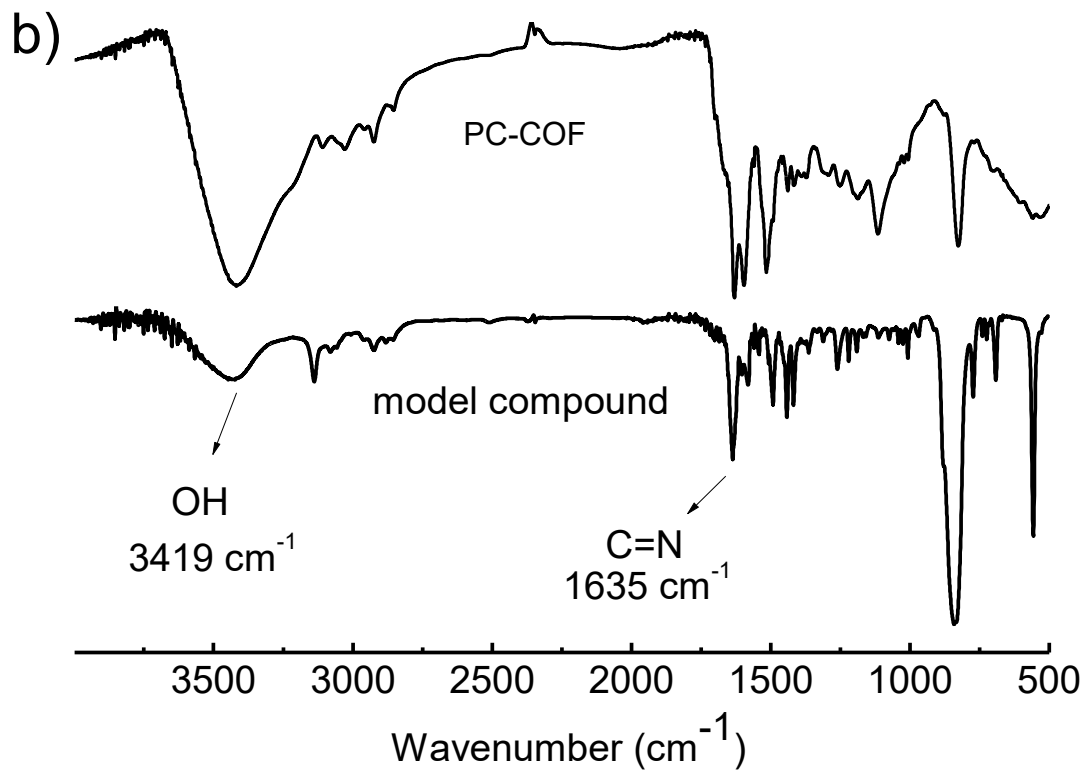
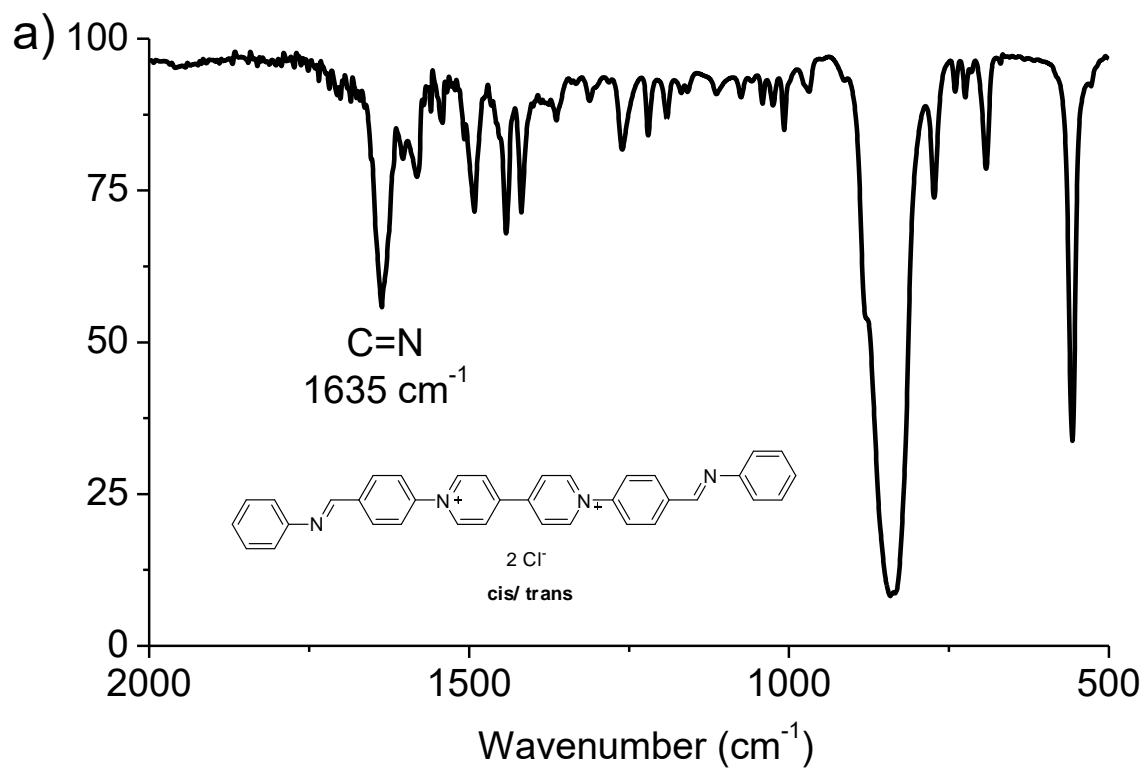


Figure S1. The FT-IR spectrum of a) model compound and b) PC-COF.

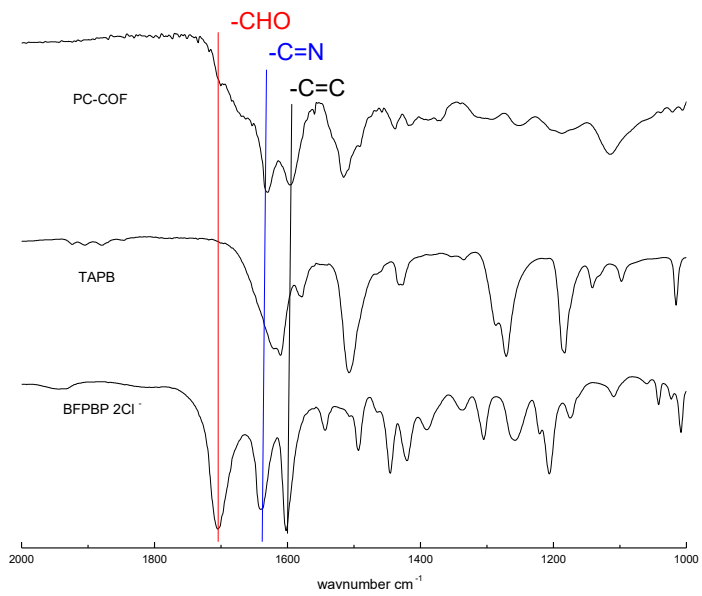


Figure S2. The FT-IR spectrum of PC-COF (upper), TBPA (middle) and BFPBP²⁺·2Cl⁻ (down).

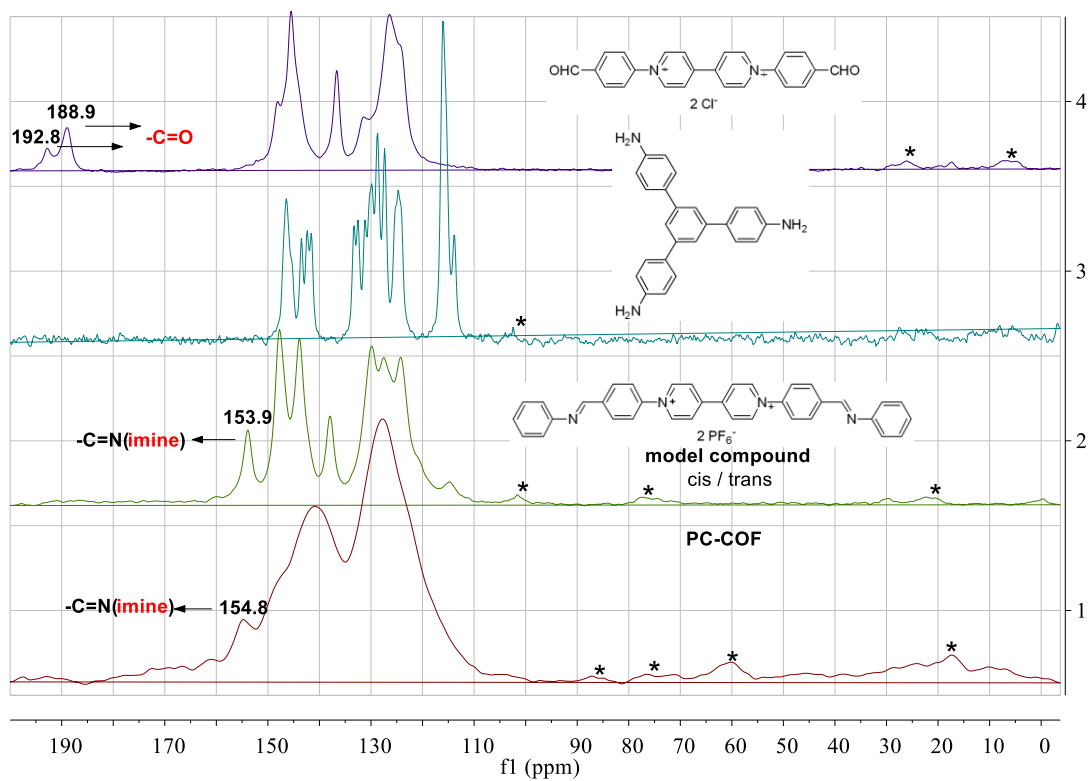


Figure S3. ¹³C NMR of BFPBP²⁺·2Cl⁻, TBPA, model compound, and PC-COF.

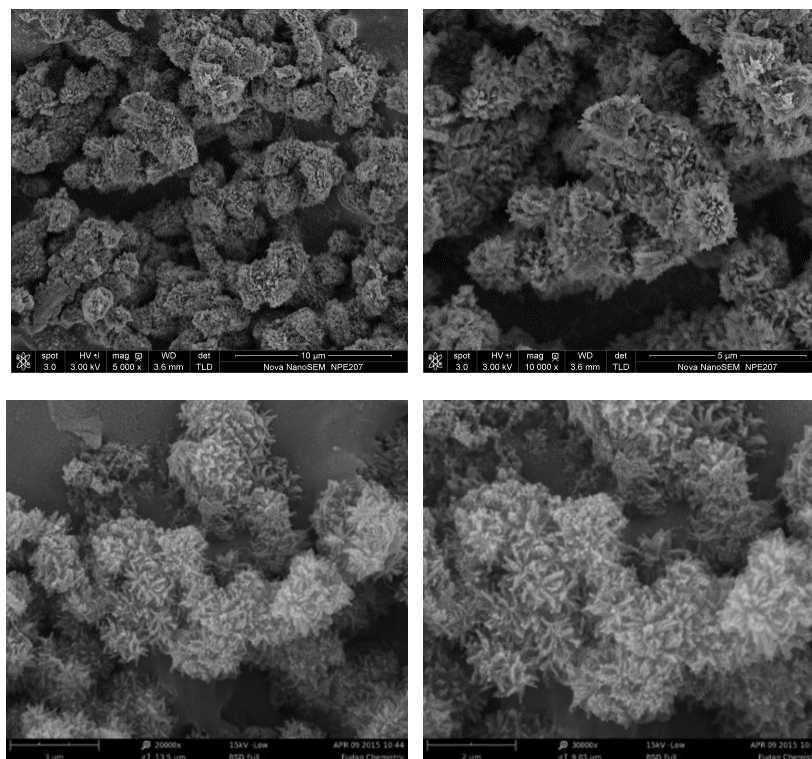


Figure S4. Field-emission SEM images of PC-COF.

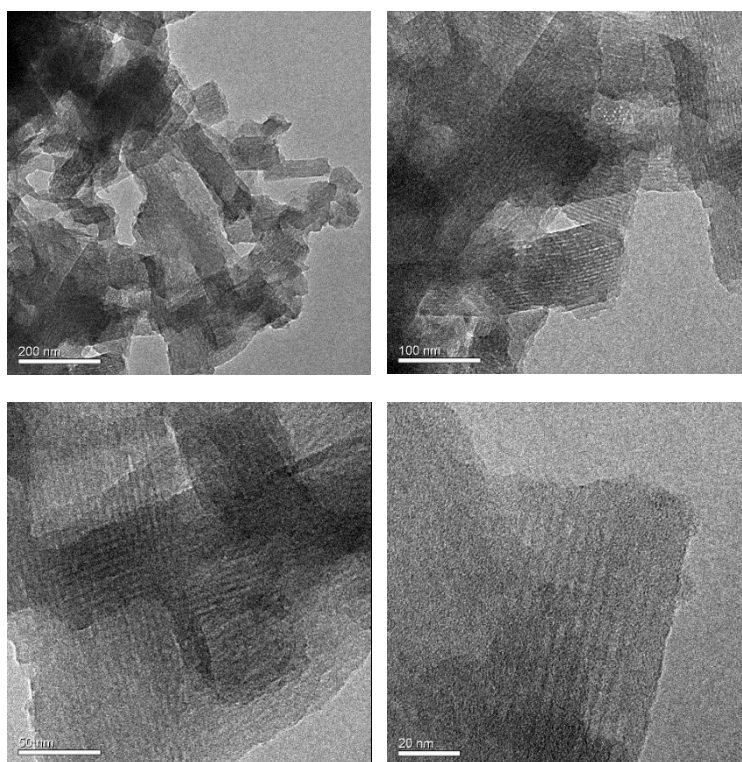


Figure S5. TEM images of PC-COF.

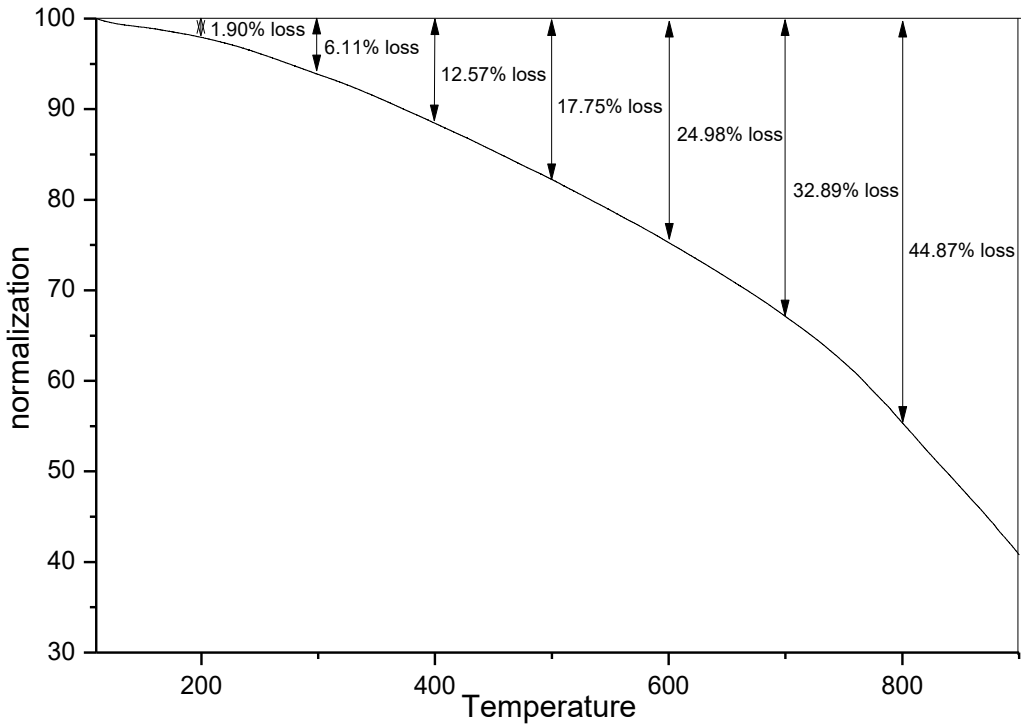


Figure S6. Thermogravimetric analysis of PC-COF.

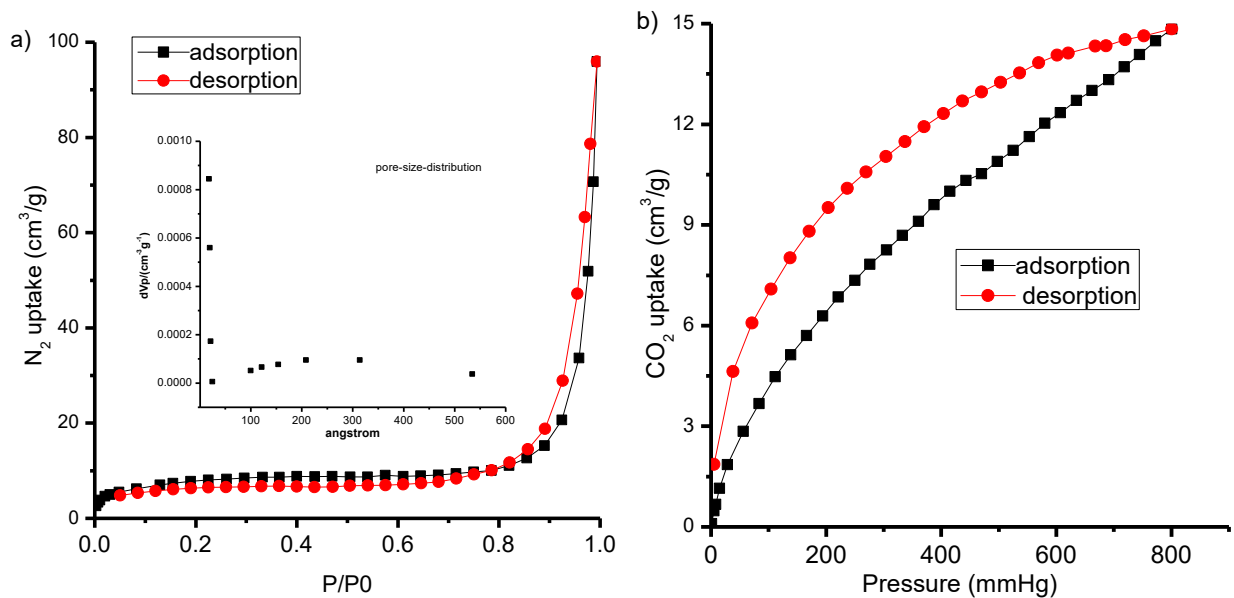


Figure S7. a) N_2 adsorption/desorption isotherms at $-196\text{ }^\circ\text{C}$ (insert pore-size-distribution) and b) CO_2 adsorption/desorption at $0\text{ }^\circ\text{C}$ of PC-COF as synthesized.

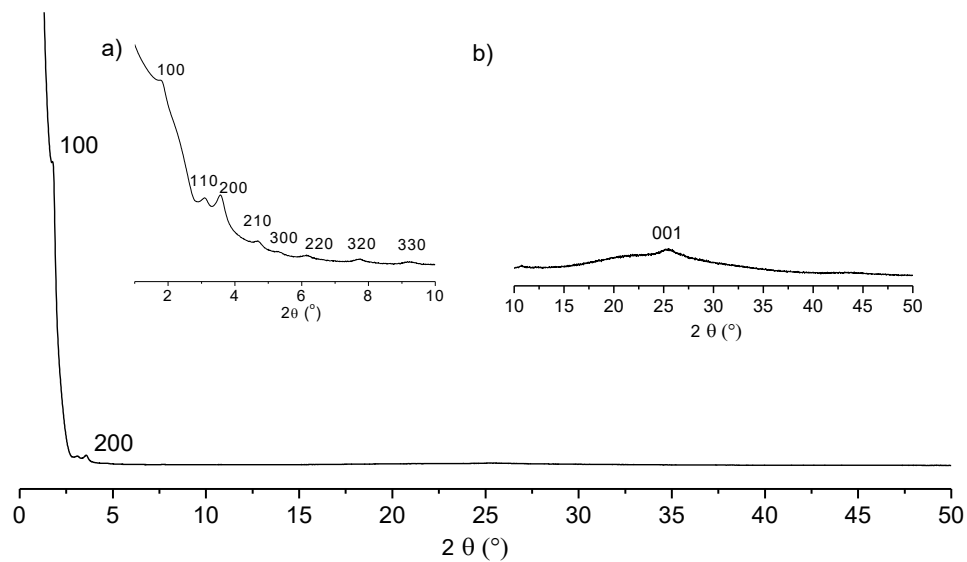


Figure S8. The PXRD profile of PC-COF.

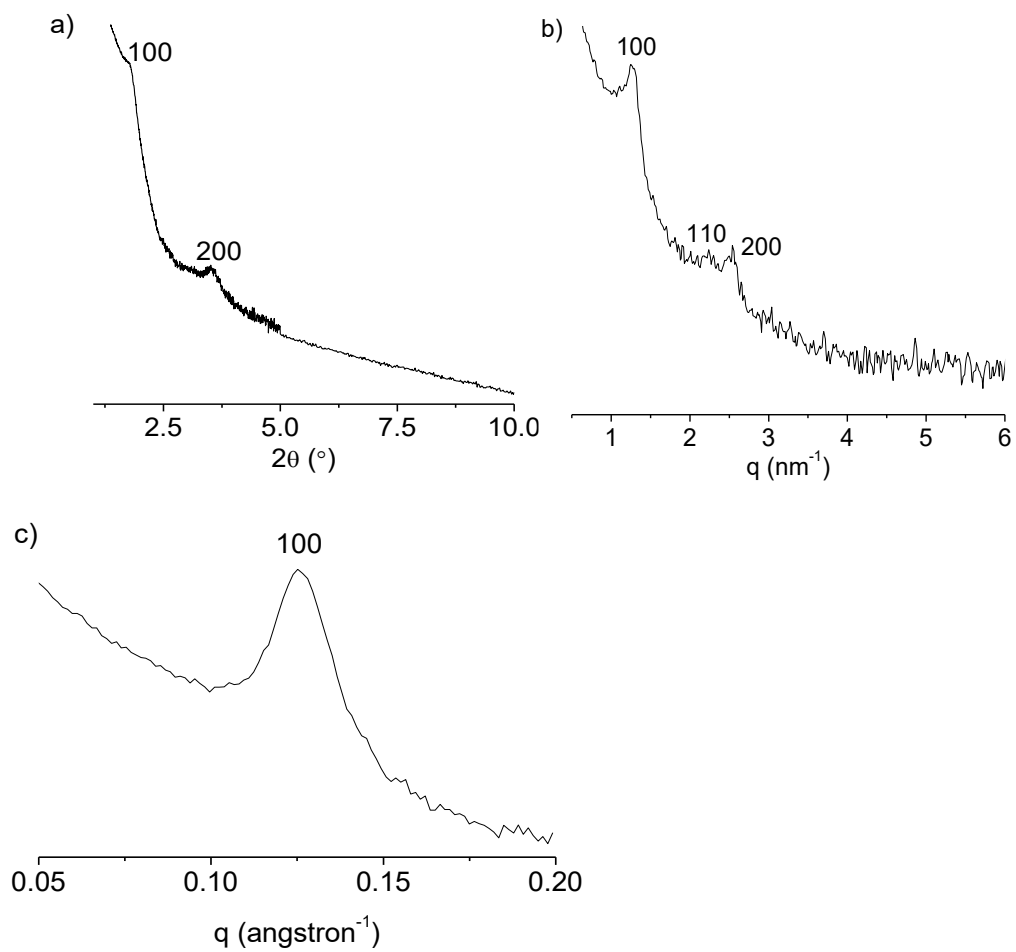


Figure S9. a) PXR, b) and c) SAXS profiles of PC-COF-2.

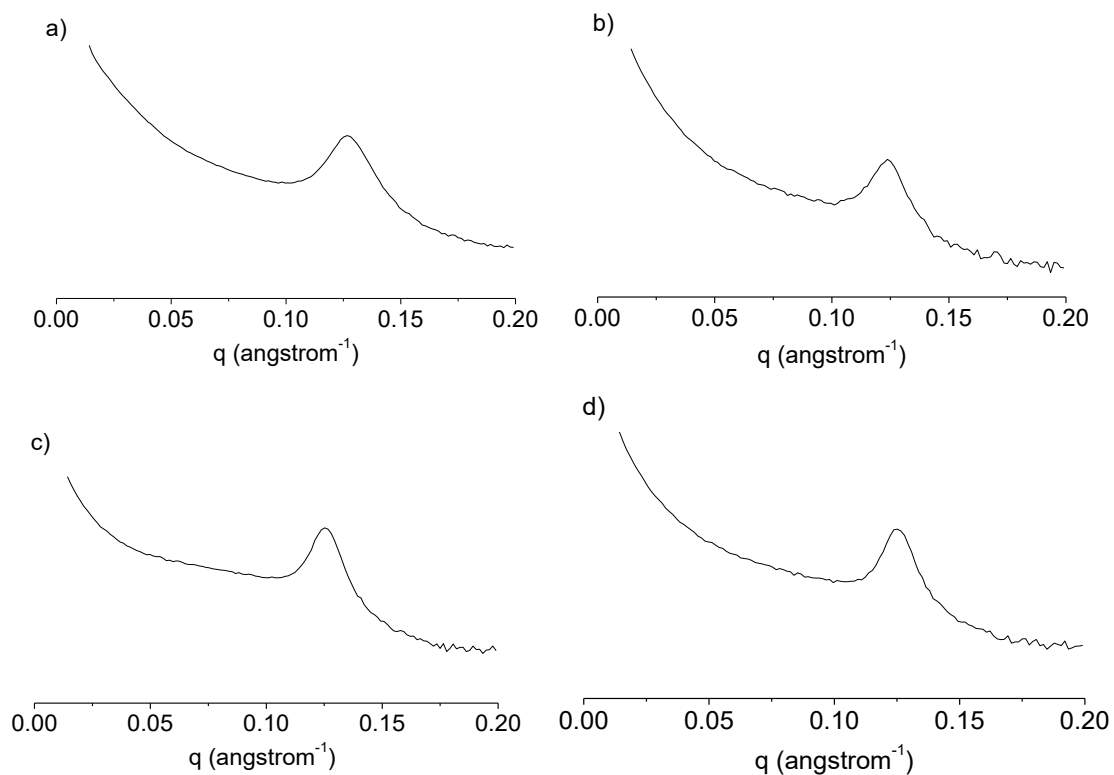


Figure S10. The SAXS profiles of **PC-COF** after soaking in water for a) 0, b) 1, c) 2, and d) 10 days. The latter three samples were obtained after being filtrated off and dried in vacuo.

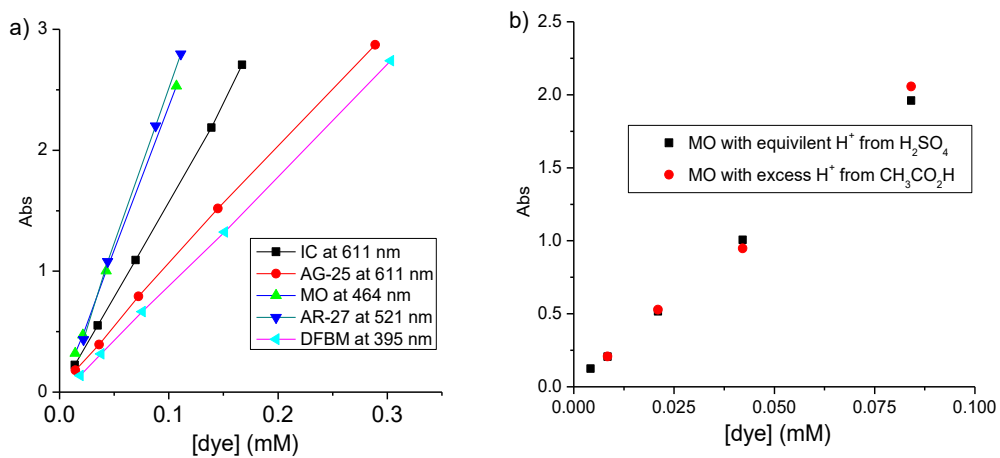


Figure S11. a) The plots of the absorbance of dyes by **PC-COF** versus the concentrations of the dyes in water. b) The absorbance of MO versus its concentrations in ethanol containing acids (2.5 mM).

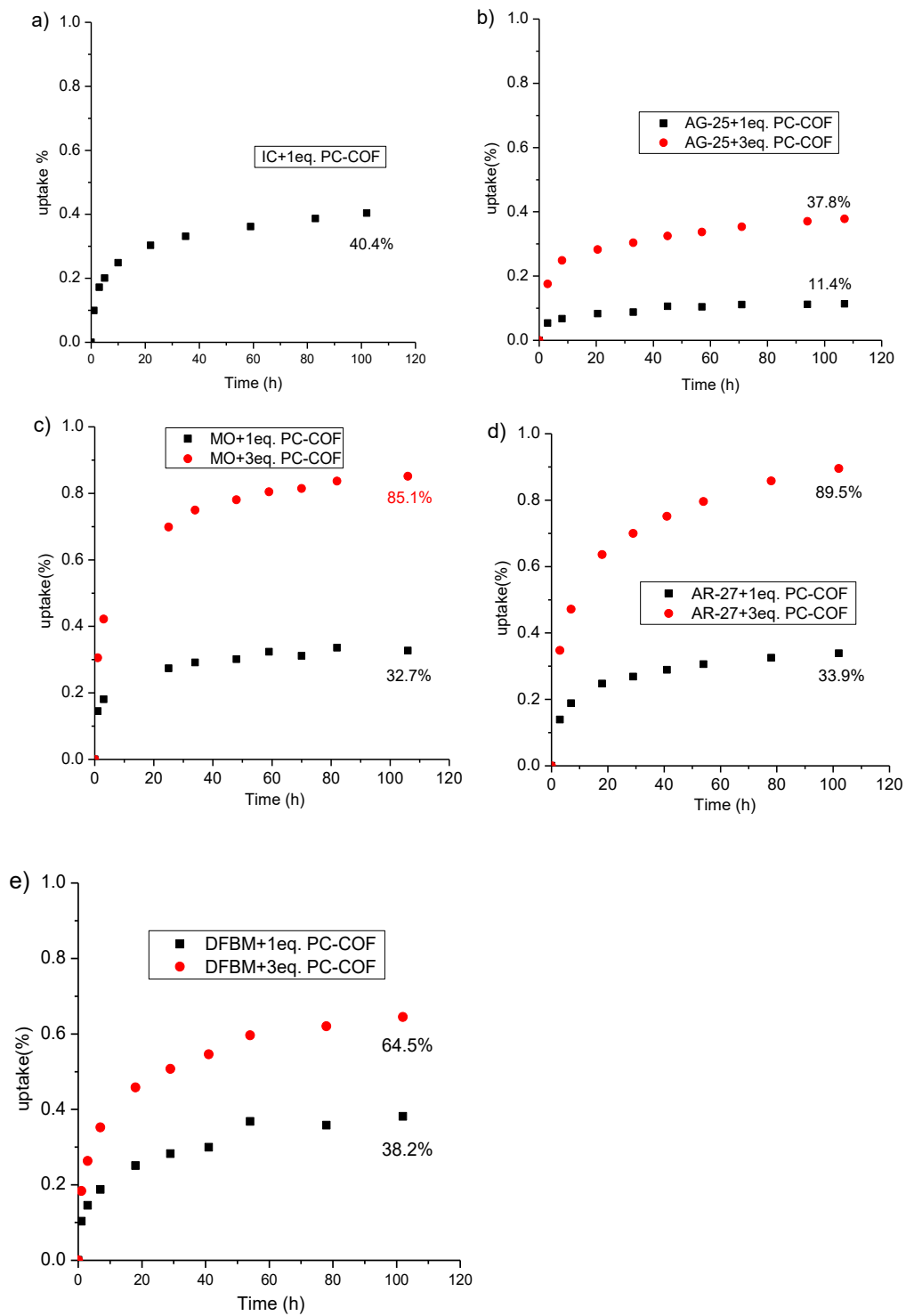


Figure S12. The uptake of organic dyes at the same charge concentration of 0.21 mM by 1 and 3 loadings of PC-COF at different times.

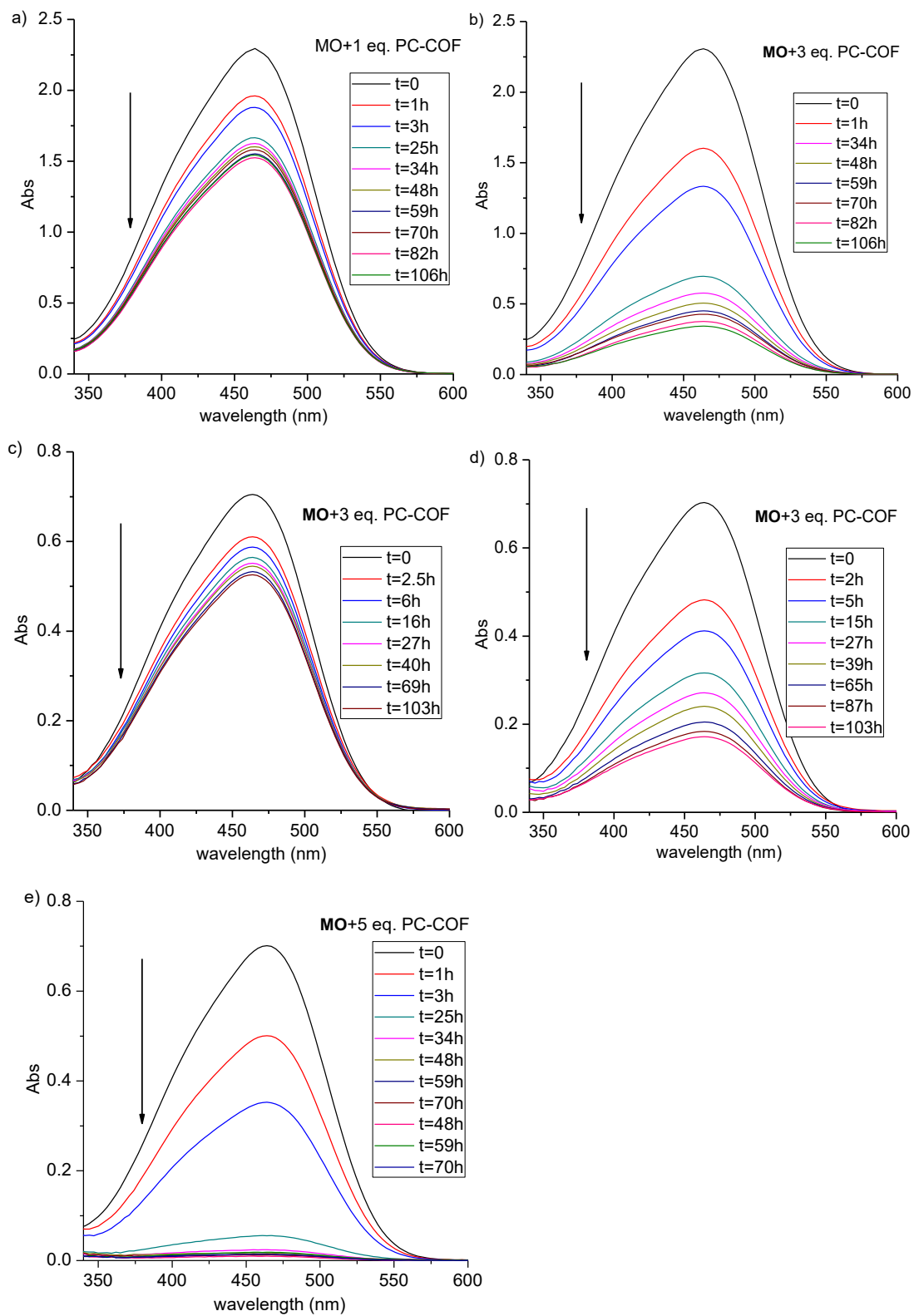


Figure S13. UV-vis spectra of MO samples at the initial concentrations of a) and b) 0.21 mM, and of c), d) and e) 0.032 mM after uptaking by different loadings of **PC-COF**.

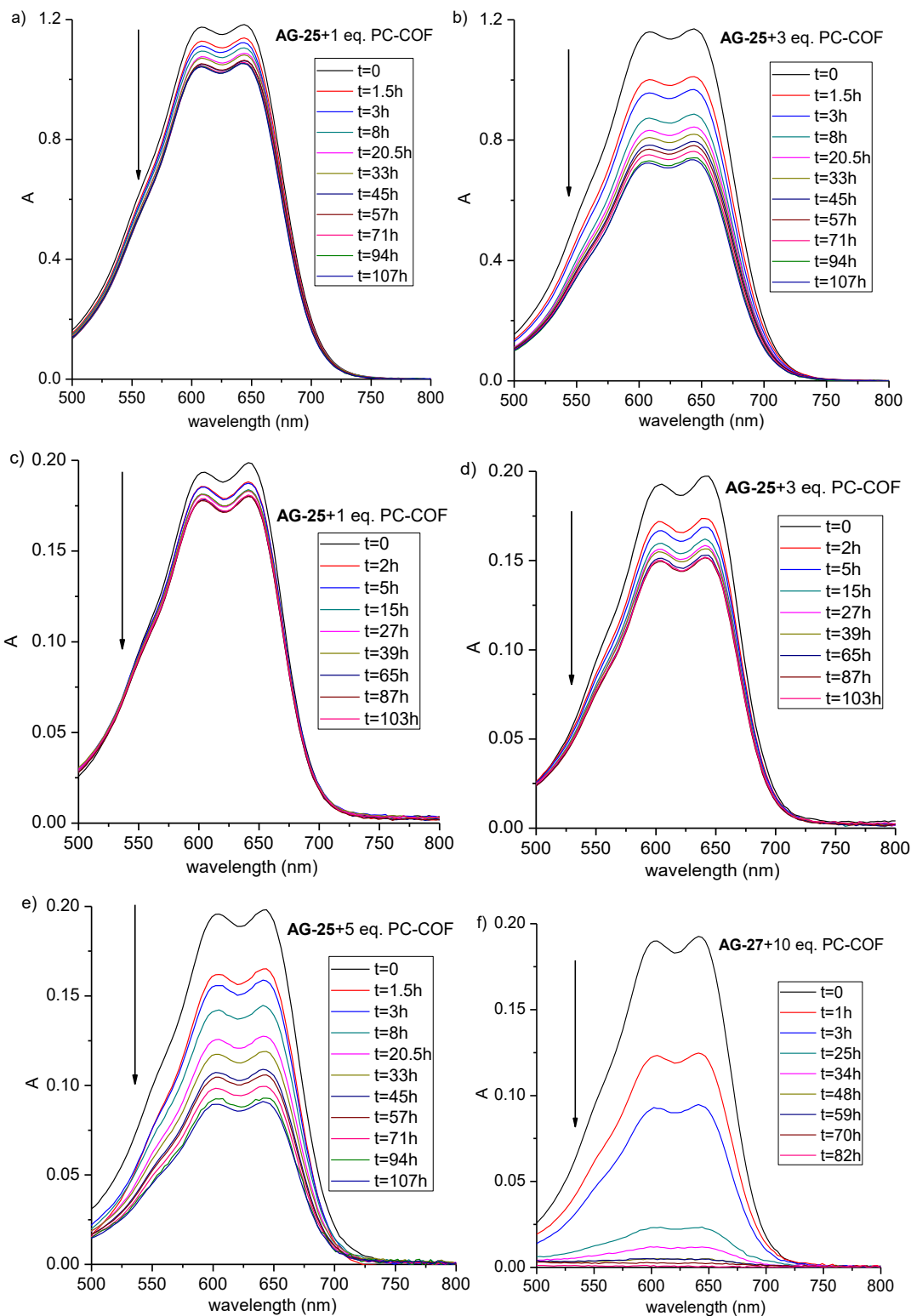


Figure S14. UV-vis spectra of AG-25 samples at the initial concentrations of a) and b) 0.11 mM, and of c), d) and e) 0.032 mM after uptaking by different loadings of **PC-COF**.

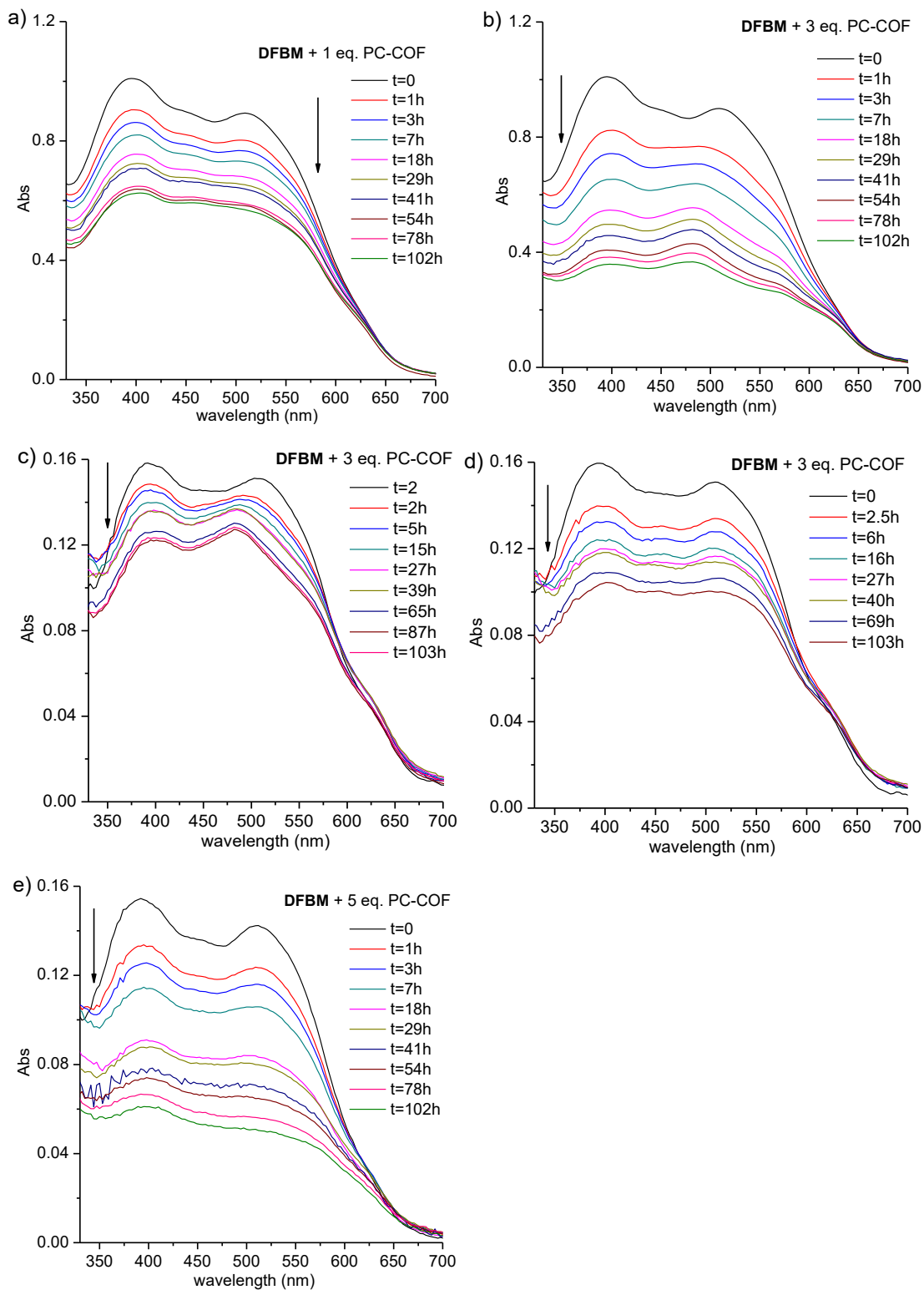


Figure S15. UV-vis spectra of **DFBM** at the initial concentrations of a) and b) 0.11 mM, and of c), d) and e) 0.032 mM after uptaking by different loadings of **PC-COF**.

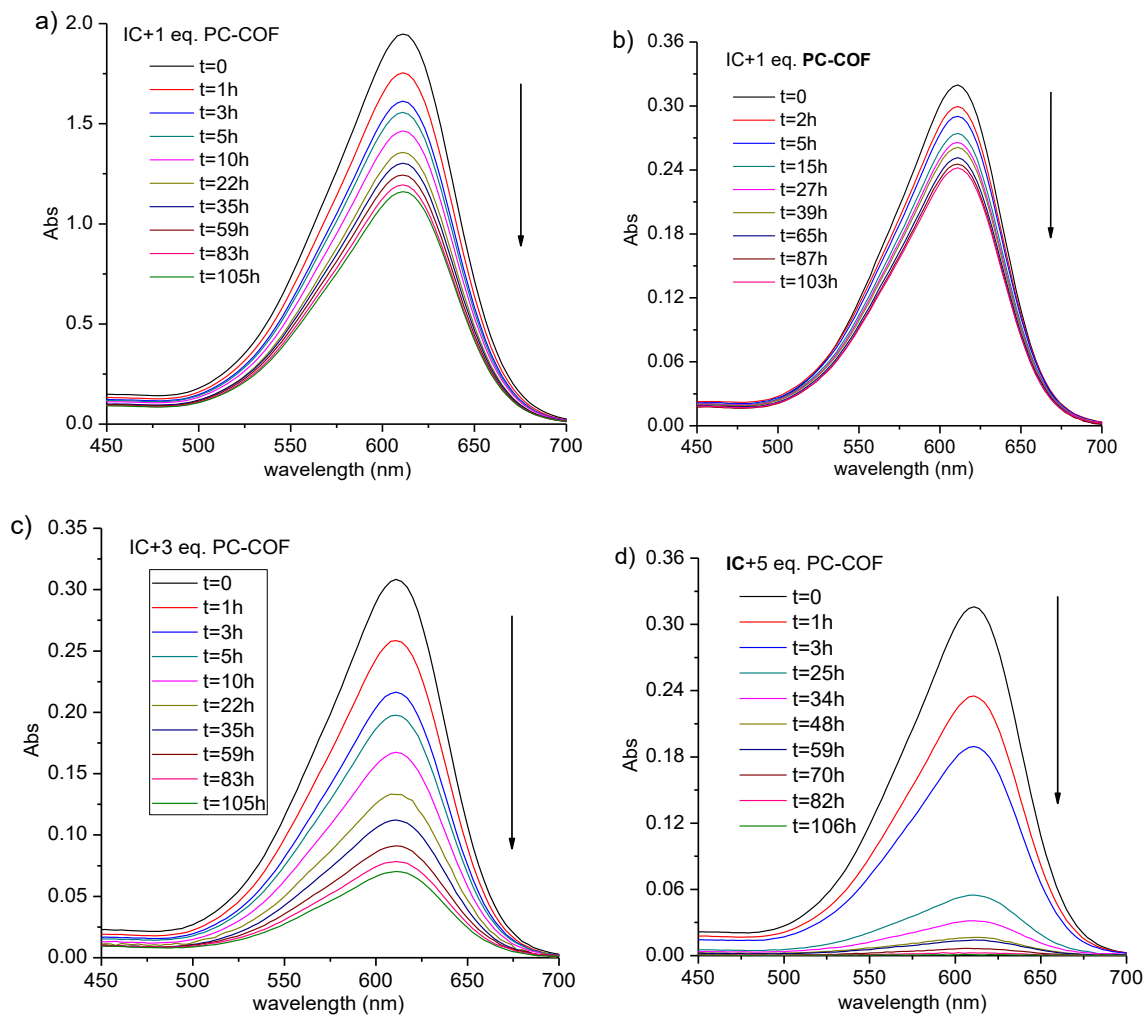


Figure S16. UV-vis spectra of IC samples at the initial concentrations of a) 0.11 mM, and of b), c) and d) 0.032 mM after uptaking by different loading of **PC-COF**.

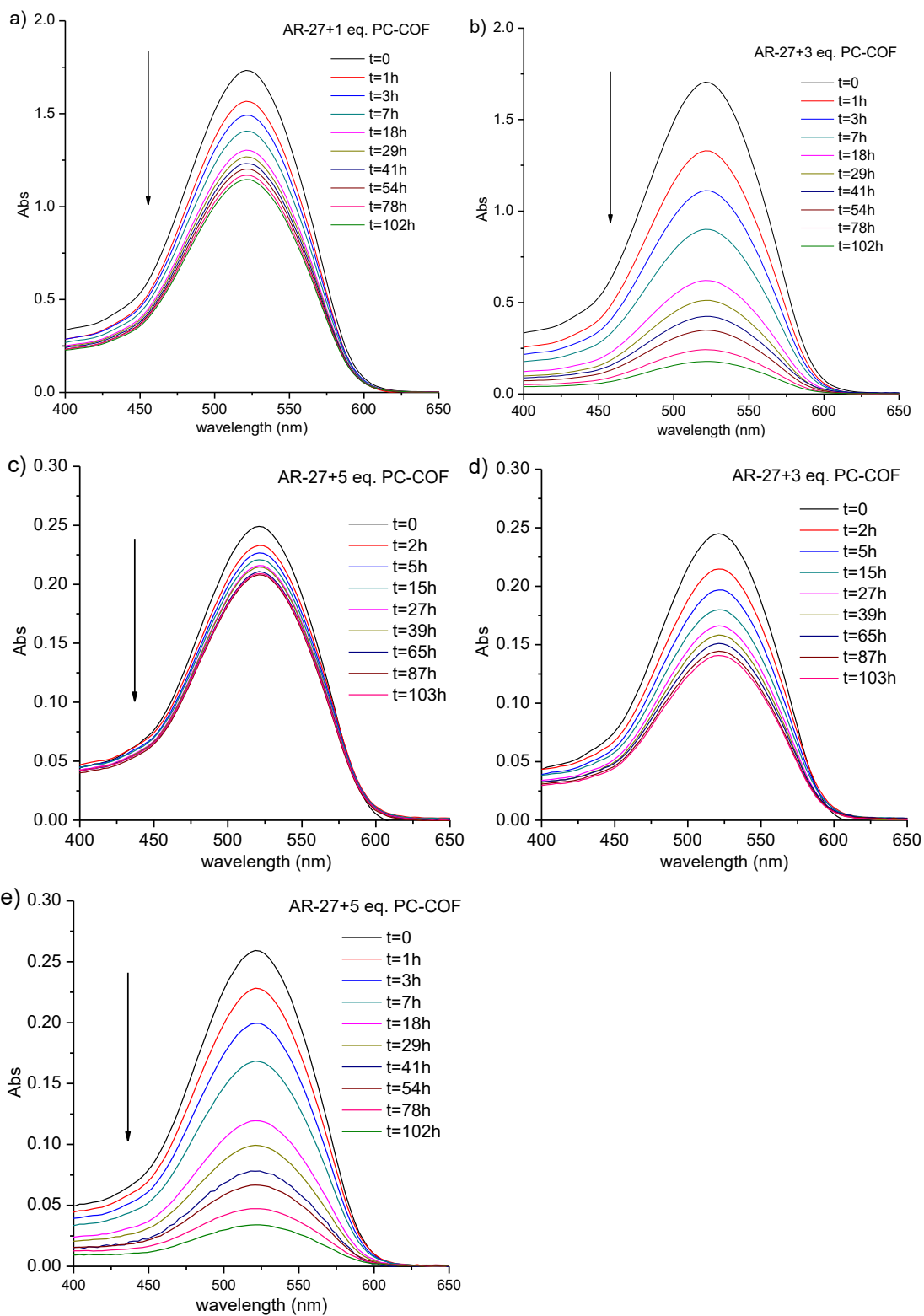


Figure S17. UV-vis spectra of AR-27 samples at the initial concentrations of a) and b) 0.07 mM, and of b), c) and d) 0.011 mM after uptaking by different loadings of **PC-COF**.

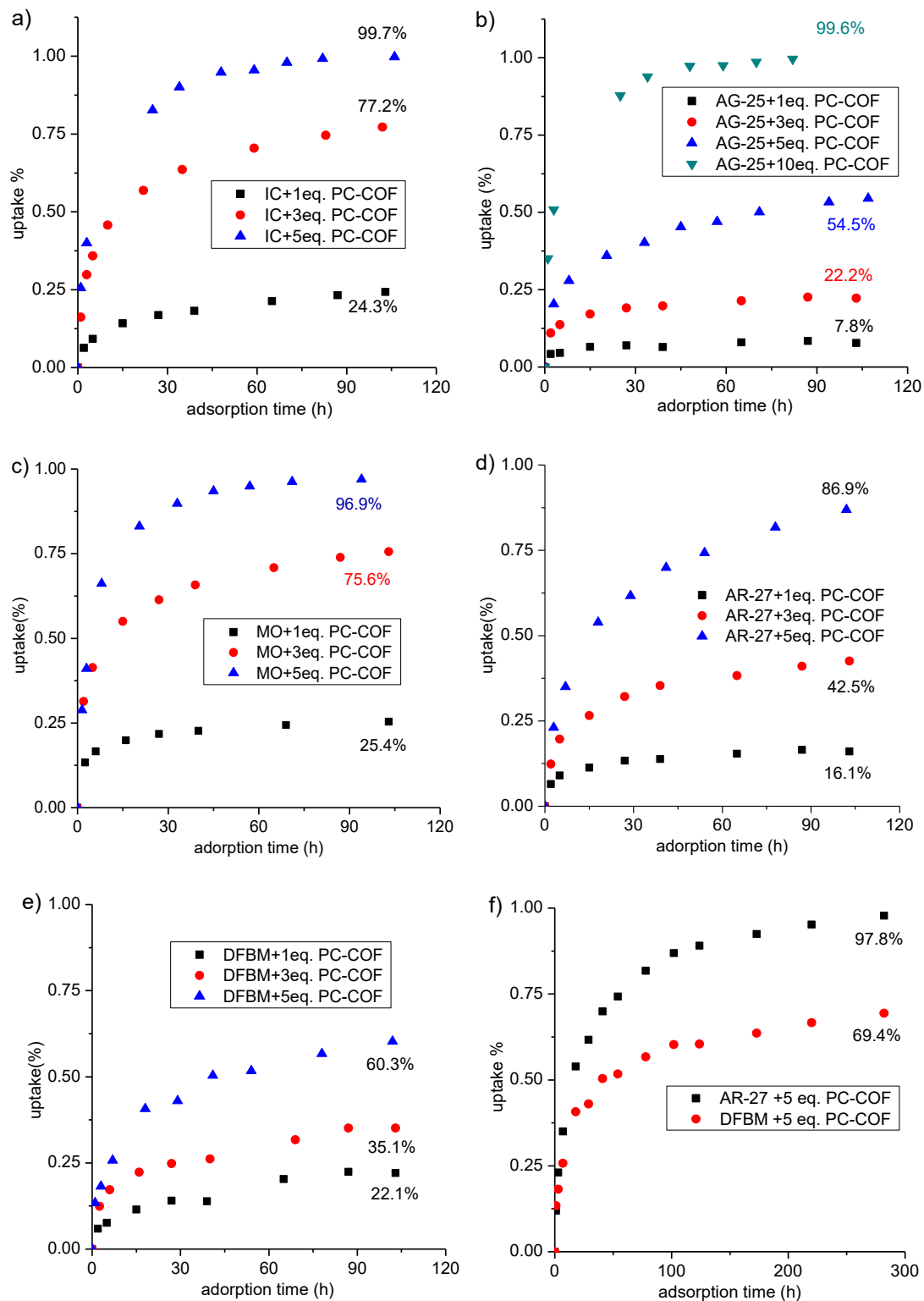


Figure S18. The normalized uptake of dyes at the same ion concentration of 0.32 mM by 1, 3, 5, and 10 loadings of PC-COF with the adsorption time being a-e) 110 h and f) 300 h.

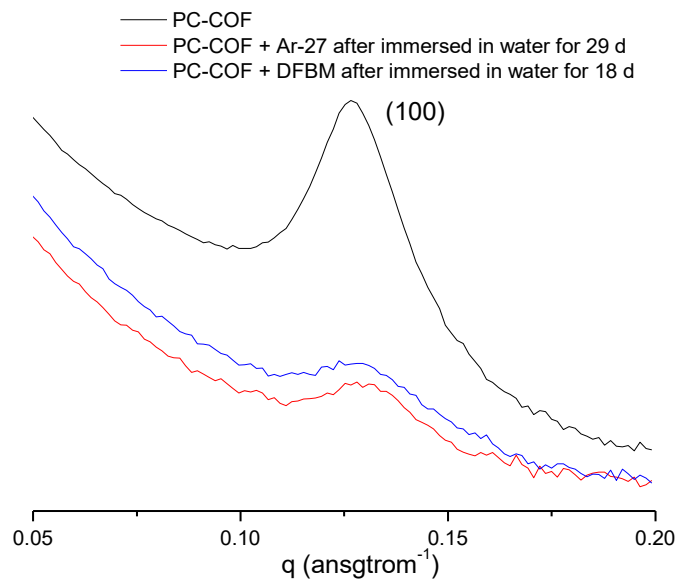


Figure S19. SAXS profiles of PC-COF before and after the uptake of AR-27 and DFBM.

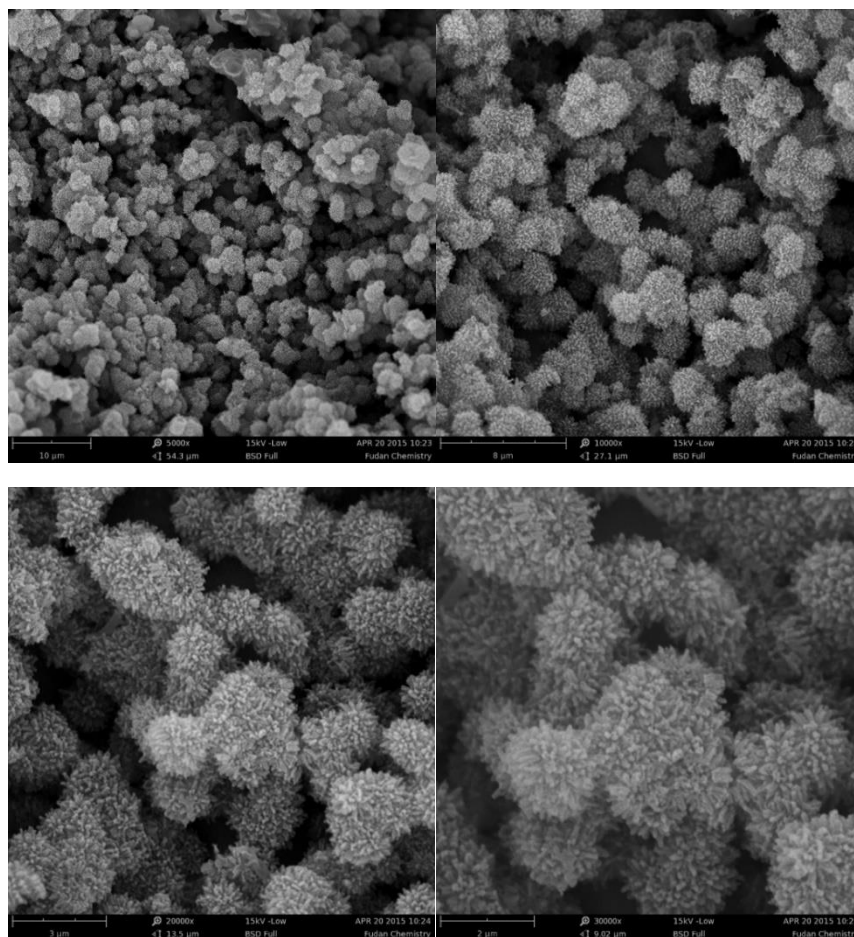


Figure S20. SEM images of PC-COF after uptaking IC from water.

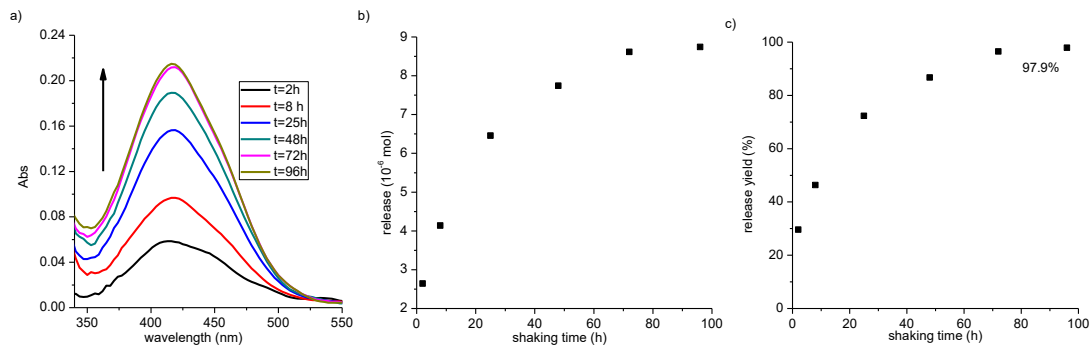


Figure S21. UV-vis spectra of MO released to ethanol containing AcOH (2.5 mM) from MO-adsorbed PC-COF.

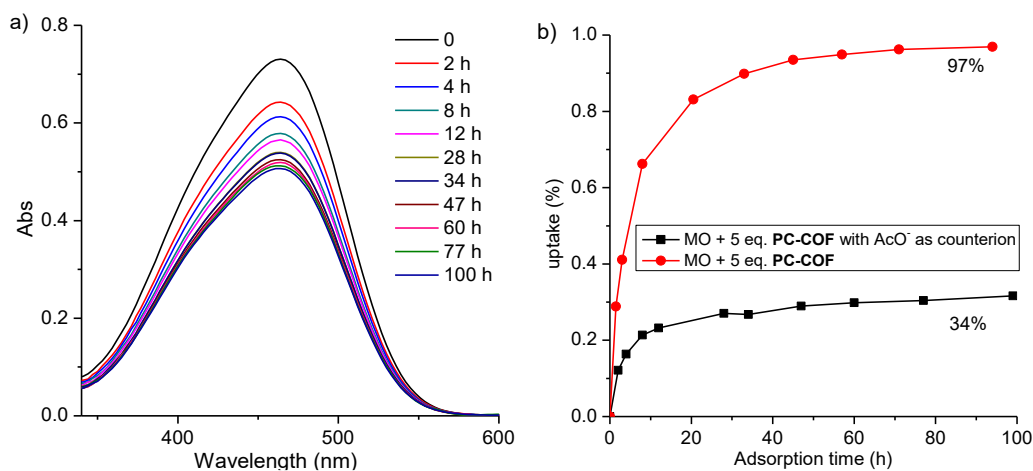


Figure S22. a) UV-vis spectra of MO (0.032 mM) of PC-COF (5 equivalent) with AcO⁻ as counterion, b) the adsorption efficiency for MO versus time.

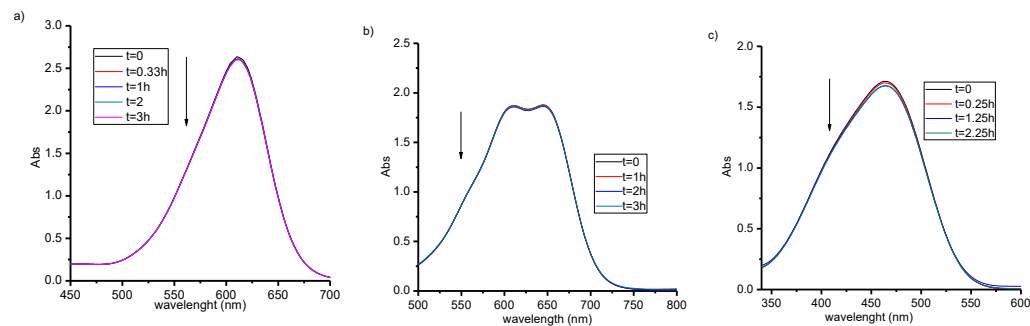


Figure 23. Time-dependent UV-vis spectra of a) IC (0.16 mM), b) AG-25 (0.16 mM), and c) MO (0.32 mM) after mixing with 1 equivalent of PC-COF-2.

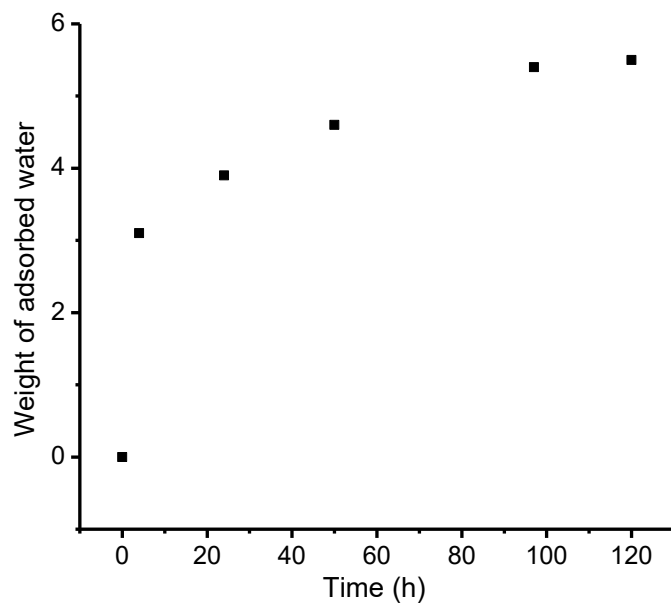


Figure S24. Water adsorption experiments of **PC-COF**. The sample (80 mg) was exposed to air of 100% relative humidity at 25 °C for 5 days. The Y-axis values represent the weight of water adsorbed by the sample.

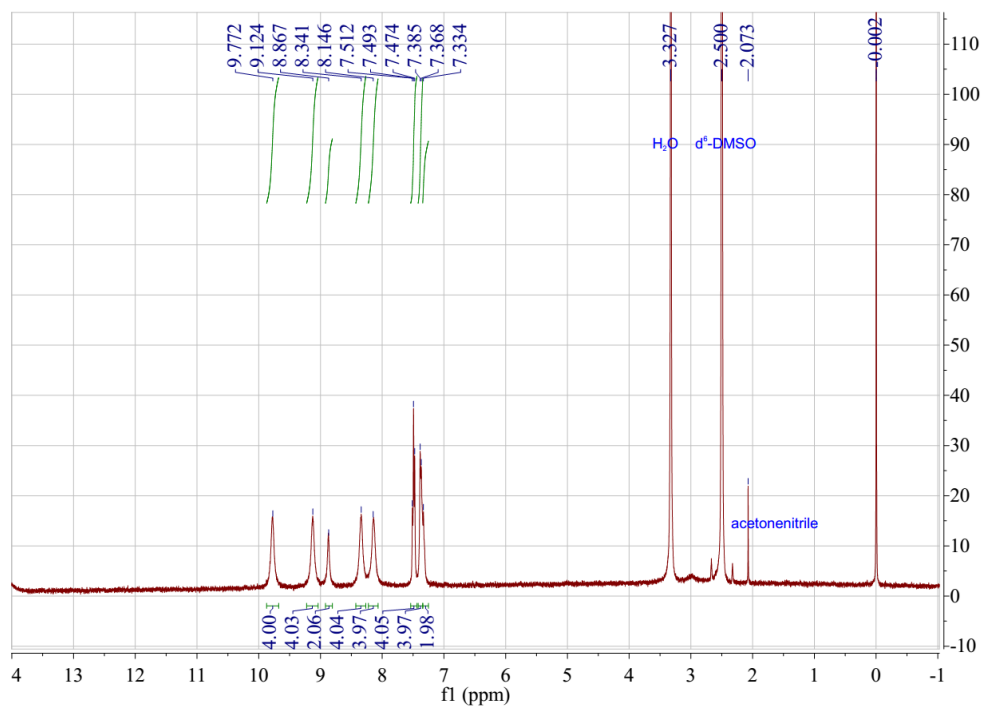


Figure S25. ¹H NMR spectrum of model compound in DMSO-d₆.

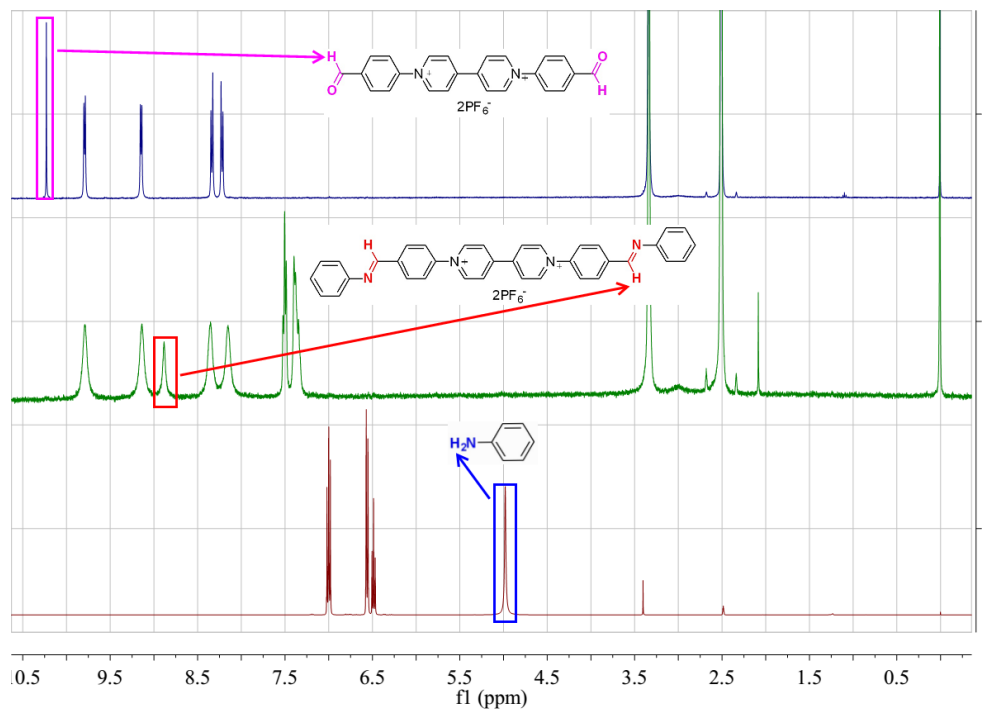


Figure S26. ¹H NMR spectrum of model compound (upper), aniline (middle), and **BFBP•2PF₆⁻** (down).

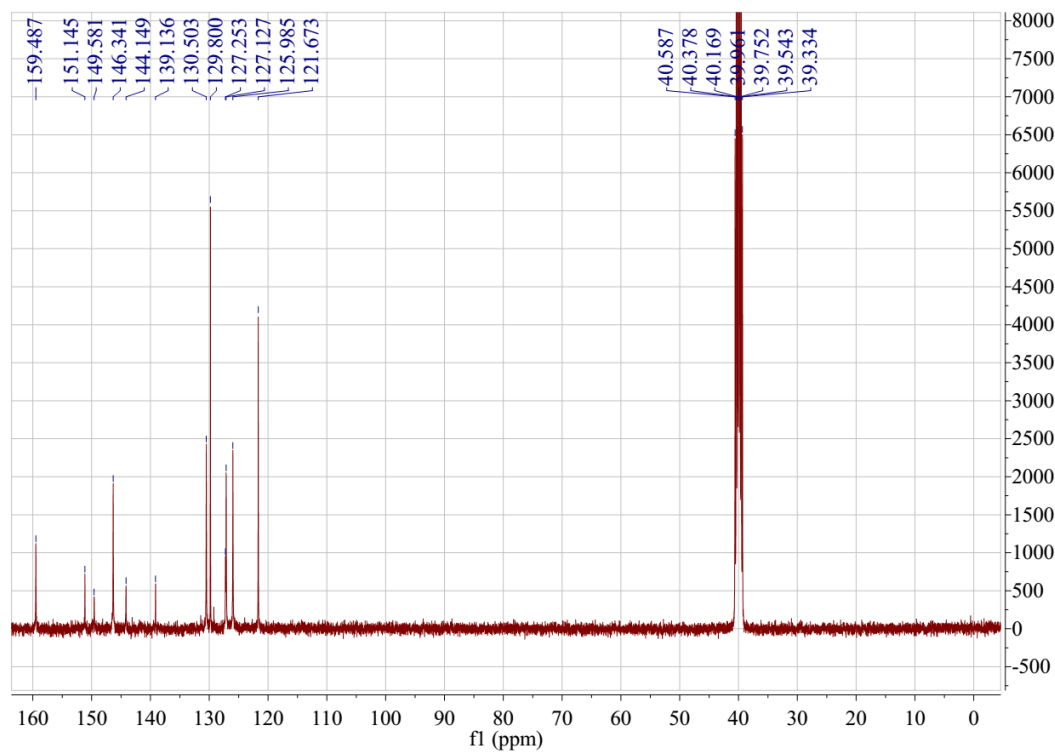


Figure S27. ¹³C NMR spectrum of model compound in DMSO-d₆.

General methods for structural simulation of PC-COF. Structure modelling of **PC-COF** was performed using the Accelrys Materials Studio 7.0 program suite.³ Geometric optimization of COF structure in classic forcefield was carried out with Forcite module, and PXRD pattern prediction was done in Reflex module. In order to simulate the electrostatic interaction between layers of the polycationic framework and anions, simple model of eclipsed (AA stacking) **PC-COF** was built and geometrically optimized in Universal forcefield with no specific charge treatment with reference to previously reported methods^{4,5} (Figure S25). The lattice was in P6/M space group, and the parameters are $a = 59.493 \text{ \AA}$, $b = 59.493 \text{ \AA}$, $c = 3.439 \text{ \AA}$, $\alpha = 90^\circ$, $\beta = 90^\circ$, $\gamma = 120^\circ$. PXRD prediction was in good agreement with experimental data even though some difference in peak strength. However, structural check revealed that inside the model, the framework was neutral and Cl⁻ anions were omitted. Thus, we considered that the above model could not represent the actual structure inside the material.

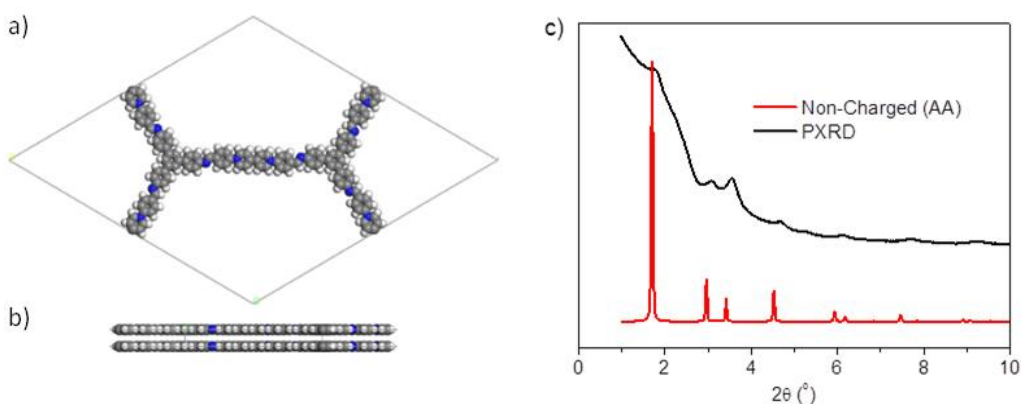


Figure S28. Simulated structure for non-charged eclipsed (AA stacking) **PC-COF** viewed from a) 001 direction, b) 110 direction, and c) the predicted PXRD pattern (down) and experimental PXRD pattern (upper).

With further investigation, different treatments were selected to incorporate charges of bipyridinium N atoms into the eclipsed **PC-COF** model. The optimization was carried out with COMPASSII forcefield, with charges specified by Gasteiger method (Gast_polygraf 1.0 parameter set) to support calculation of 4-valent nitrogen, which was used in following models without specification (Figure S26). The lattice parameters were $a = 58.281 \text{ \AA}$, $b = 58.929 \text{ \AA}$, $c = 19.999 \text{ \AA}$, $\alpha = 89.958^\circ$, $\beta = 89.840^\circ$, $\gamma = 119.792^\circ$, and Cl⁻ anions were put in random coordination in the pores, thus the symmetry group changed to P1. The resulting structure gave a lattice with a c parameter of $\sim 20 \text{ \AA}$ but still did not reach a convergence, resulting in a 001 signal at $\sim 4.4^\circ$, which did not match the experimental data. This indicated a strong repulsion between positive charges of the stacked layers of **PC-COF**.

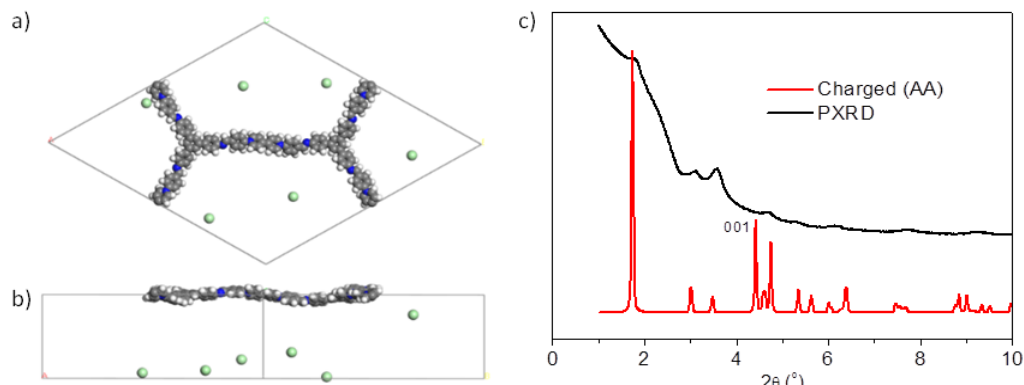


Figure S29. Simulated structure of charged eclipsed (AA stacking) **PC-COF** viewed from a) 001 direction, b) 110 direction, and c) the predicted PXR pattern and the experimental PXR pattern.

Staggered (AB stacking) structure of honeycomb COFs, with the same stacking pattern as graphite, was considered to be able to release the direct repulsion between cations of paralleled layers. Optimization with the same treatment as shown above gave the structure of $c = 7.043 \text{ \AA}$, which was consistent to the experimental data, but the relative intensity of peaks between $1 \sim 10^\circ$ did not match ideally (Figure S27), indicating this might not be the best structure. However, it was observed that the randomly placed Cl^- anions were drawn to the framework, “harboring” in between positively charged bipyridinium -N atoms of adjacent A (or B) layers, causing an interlayer distance of $\sim 7 \text{ \AA}$. The N-Cl distances were measured as 3.31 \AA and 5.14 \AA (average). This indicated that counter ions harboring close to or inserted in between layers of the framework might alleviate the electrostatic repulsion and stabilize the structure to some extent.

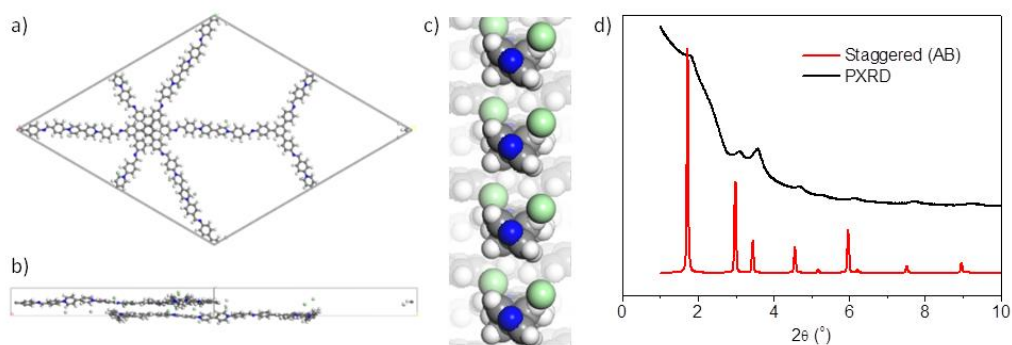


Figure S30. Simulated structure of charged staggered (AB stacking) **PC-COF** viewed from a) 001 direction, b) 110 direction, and c) 1,-1,0 direction (gray: C, white: H, blue: N, green: Cl), and d) the predicted PXR pattern and the experimental PXR pattern.

The above result was introduced back to the eclipsed model of **PC-COF**, and the interlayer distance was decreased to 6.5 \AA , which was a large improvement but still inconsistent with the observed distance. Small

arbitrary shift of 4.44 Å was tried according to similar treatment of a formerly reported COF model,⁴ leading to a model shown in Figure S28, with the lattice parameters of $a = 58.100$ Å, $b = 60.229$ Å, $c = 6.944$ Å, $\alpha = 91.388^\circ$, $\beta = 92.500^\circ$, $\gamma = 121.849^\circ$. The shift was drawn back by the strong stacking of TAPB residues. However, probably because of its perturbation to the symmetry, the BP linkers were slightly bent (measured 156.6°) sideward and the interlayer distance was 3.47 Å. This model showed a favored conformation of π - π stacking, where the bipyridinium rings packed sideward with the C-H bonds of one stretching towards center of another, and Cl⁻ anions were close aside to neutralize the charge repulsion. From (110) view of the simulated crystal, the components actually formed two bipyridinium-Cl⁻ bipyridinium arrays bound by π - π sideward stacking. The N-Cl distance were measured to be 3.36-3.67 Å, similar to those of the staggered model. To determine whether this pattern was a coincidence, larger shift and arbitrary shift directions of simulation input were tried with the same algorithm, but they converged to almost identical ones like the above. We therefore proposed that this was a favored conformation of **PC-COF**.

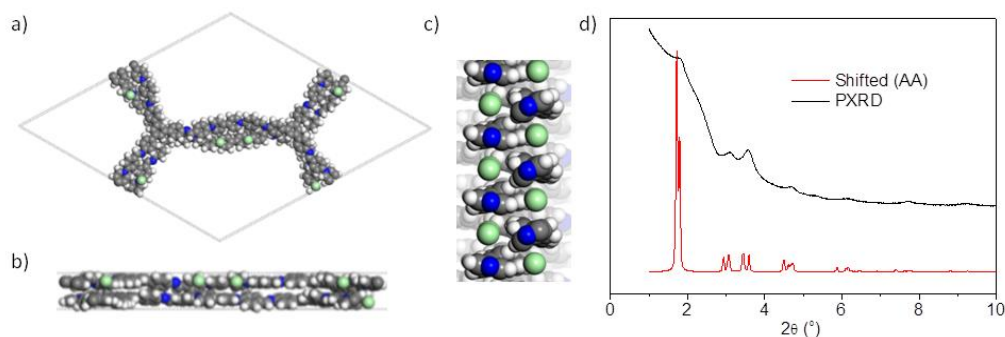


Figure S31. Simulated structure of charged eclipsed (slipped AA stacking) **PC-COF** from a) 001 direction, b) 110 direction, and c) 1, -1, 0 direction (gray: C, white: H, blue: N, green: Cl) and d) its predicted PXR patterns with real ones.

References

- 1) Zhao, Y.; Li, J.; Chun, C.; Yin, K.; Ye, D.; Jia, X. *Green Chem.* **2010**, *12*, 1370.
- 2) Chen, L.; Wang, H.; Zhang, D.-W.; Zhou, Y.; Li, Z.-T. *Angew. Chem. Int. Ed.* **2015**, *54*, 4028.
- 3) Accelrys, Material Studio Release Notes, Release 7.0, Accelrys Software, San Diego 2013.
- 4) Guo, J.; Xu, Y.; Jin, S.; Chen, L.; Kaji, T.; Honsho, Y.; Addicoat, M. A.; Kim, J.; Saeki, A.; Ihee, H.; Seki, S.; Irle, S.; Hiramoto, M.; Gao, J.; Jiang, D. *Nat. Commun.* **2013**, *4*, 3736.
- 5) Dogru, M.; Sonnauer, A.; Gavryushin, A.; Knochel, P.; Bein, T.; *Chem. Commun.* **2011**, *47*, 1707.